**Research Article** **Open Access**

Teo Asplund*, Cris L. Luengo Hendriks, Matthew J. Thurley, and Robin Strand

# Mathematical Morphology on Irregularly Sampled Data in One Dimension

https://doi.org/10.1515/mathm-2017-0001
Received June 26, 2017; accepted October 17, 2017

**Abstract:** Mathematical morphology (MM) on grayscale images is commonly performed in the discrete domain on regularly sampled data. However, if the intention is to characterize or quantify continuous-domain objects, then the discrete-domain morphology is affected by discretization errors that may be alleviated by considering the underlying continuous signal. Given a band-limited image, for example, a real image projected through a lens system, which has been correctly sampled, the continuous signal may be reconstructed. Using information from the continuous signal when applying morphology to the discrete samples can then aid in approximating the continuous morphology. Additionally, there are a number of applications where MM would be useful and the data is irregularly sampled. A common way to deal with this is to resample the data onto a regular grid. Often this creates problems where data is interpolated in areas with too few samples. In this paper, an alternative way of thinking about the morphological operators is presented. This leads to a new type of discrete operators that work on irregularly sampled data. These operators are shown to be morphological operators that are consistent with the regular, morphological operators under the same conditions, and yield accurate results under certain conditions where traditional morphology performs poorly.

**Keywords:** Irregular sampling, One-dimensional, Continuous morphology.

## 1 Introduction

Traditionally, mathematical morphology on digital grayscale images is computed by increasing/decreasing the value of samples in a regular grid, based on the fit of a discrete structuring element (SE) [16]. However, if the goal is to approximate the result of applying morphology to a continuous signal that has been sampled to generate the digital image, there are a number of issues. These issues, we claim, may be alleviated by making use of morphology on irregularly sampled signals (or *irregular morphology*).

Specifically, the motivation behind moving to irregular morphology stems mainly from the following observations: A continuous-domain band-limited signal (for example, a real image projected through a lens system [10]) can be represented by regular sampling at a sufficiently high frequency, as shown by Nyquist and Shannon [14, 17], e.g. as a digital image. However, transforming the continuous band-limited signal by a continuous morphological operator, will generally introduce unbounded frequencies, therefore the transformed signal will no longer be band-limited and thus not representable on the regular sampling grid.

Since the continuous, band-limited signal can be reconstructed from a correctly sampled discrete signal [14, 17], one should be able to better approximate the continuous morphological operators. In this paper, which builds on a previous paper by the authors [3], we propose an algorithm to compute the dilation, making use of irregular sampling, which can alleviate the problems discussed above. Irregular sampling does not

***Corresponding Author: Teo Asplund:** Centre for Image Analysis, Uppsala University, Uppsala, Sweden. E-mail: teo.asplund@it.uu.se
**Cris L. Luengo Hendriks:** Flagship Biosciences Inc., Westminster, Colorado, USA. E-mail: luengo@ieee.org
**Matthew J. Thurley:** Luleå University of Technology, Luleå, Sweden. E-mail: matthew.thurley@ltu.se
**Robin Strand:** Centre for Image Analysis, Uppsala University, Uppsala, Sweden. E-mail: robin@cb.uu.se

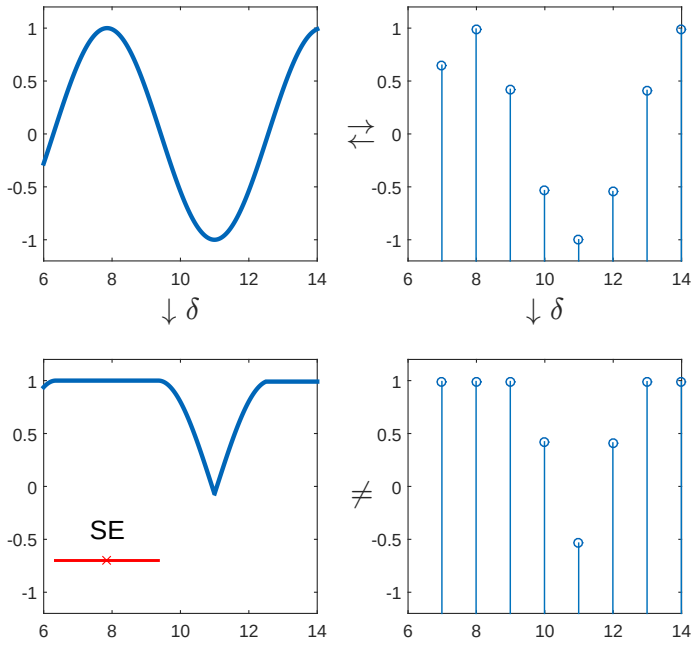


**Figure 1:** Top left: a band-limited continous signal. Top right: a sampling of the band-limited continous signal. Bottom left: a dilation of the continuous signal. Note the cusp, which introduces unbounded frequencies. Bottom right: discrete dilation of the sampled signal. Note that the sampling density remains the same, even though higher frequencies are now present in the continuous signal. The correspondence between the discrete and continuous domain has been broken. The SE is indicated in red.

follow Nyquist-Shannon sampling theory, and opens up possibilities of representing discontinuous signals and discontinuous derivatives, as required to represent the output of the continuous morphological operators. The proposed approach will still, no doubt, be unable to perfectly represent continuous morphology, since no discrete set of samples can represent a continuous-domain signal without imposing limitations on said signal. However, experiments in this paper show that the proposed irregular morphology may indeed better approximate continuous morphology.

Allowing for irregular sampling, interestingly, enables varying the sampling density over the signal. Therefore smooth parts of the continuous signal can be sampled less densely (the operators often produce plateaus, which should not need as many samples to represent accurately) than parts of the signal that vary quickly (such as the cusp in Fig. 1), which need to be sampled more frequently. This should improve the approximation of the continuous signal without exploding the number of samples in the output.

Moreover, since the structuring element is no longer restricted by a sampling grid, in 1D the length of the SE is no longer necessarily an integer, allowing for subpixel accuracy (see Fig. 2(a)). Additionally, although not explored in this paper, allowing for irregular sampling makes possible some other avenues of potential improvement, namely:

- Since the morphological operators depend on extrema in the continuous signal, which are not necessarily sampled, even if the sampling frequency is adequate, it should be beneficial to incorporate samples taken at positions of the signal where such extrema occur. If irregularly sampled signals are allowed, we may preprocess the input and add samples at local maxima/minima (Fig. 3). This is not possible for a regularly sampled signal, since one may not freely insert samples at arbitrary positions, without increasing the sampling density everywhere.
- In 2D, the sampling grid means that the SE may not be rotationally invariant. Allowing for irregular sampling enables sampling of the SE exactly along its edge (see Fig. 2(b)).

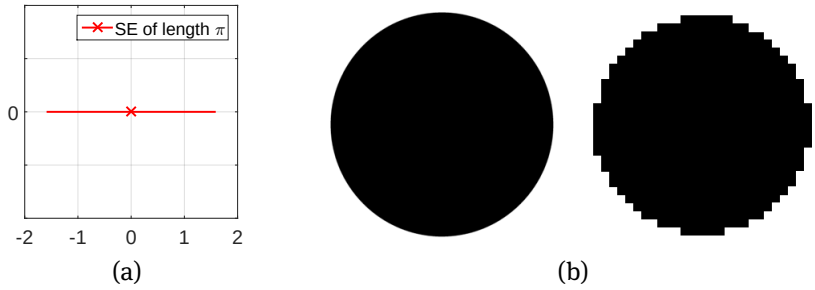


**Figure 2:** (a) A one-dimensional structuring element. The SE is of length $\pi$, however, the sampling grid does not allow a discrete SE of the same length. Instead, the grid in this example leads to a corresponding discretized SE of length two. (b) A continuous disc shaped SE and its discretized counterpart.

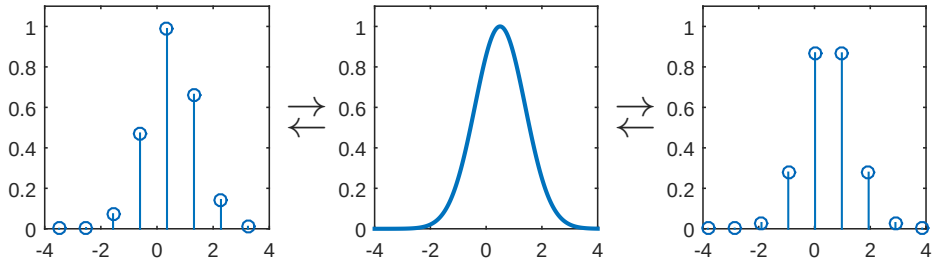


**Figure 3:** Middle: Continuous band-limited signal. Left and right: two equally dense samplings of the band-limited signal. Note that on the left one of the samples is close to the maximum, while none of the samples on the right is.

- Irregular morphology makes it possible to apply MM to signals which are irregularly sampled to begin with, instead of the common approach of preprocessing the input by interpolating the samples onto a regular grid before applying regular discrete morphology, which may cause problems if there are large holes in the data.

Previously Brockett and Maragos [5] developed partial differential equations whose evolution can compute continuous morphology in the discrete domain. Several papers were built upon this idea [4, 15, 19], however, in general, the result is represented on a regular grid and therefore cannot represent the continuous operators well (for previously mentioned reasons), at least not without using a very dense grid. The PDE based approaches also often have a tendency to blur the objects, especially near edges [4]. Moreover, these approaches are slow compared to regular discrete morphology [20].

There has also been some work done on morphology on irregularly sampled data, e.g., the thesis by Thurley [18], which proposes computing morphological operators by shifting sample points vertically, based on continuous structuring elements. Since the transformed signal is sampled at the same points as the original signal, this method suffers from similar problems as those of the regular, discrete operators.

In a paper from 2014, Calderon and Boubekeur [7] propose a method of applying morphology to 3D point clouds sampling a surface, by projecting points such that dilations, erosions, openings, and closings are sampled.

Finally, Luengo Hendriks and van Vliet [11] propose one-dimensional operators that apply continuous morphology by interpolating sampled signals.

In the following sections, we will consider only one-dimensional morphology, unless otherwise specified. We will expand on our previous paper [3] and show that the proposed algorithm does in fact, compute an actual dilation, under certain conditions. We also experimentally show that the algorithm yields a good approximation of continuous morphology, even when such conditions are not fulfilled.

# 2 Irregular Morphology

We will refer to a morphological operator on irregularly sampled signals as *irregular*.

To deal with the problems of traditional morphology discussed in the previous section, we propose a new approach to morphology based on duplicating, shifting, and deleting nodes. The proposed operations use a continuous structuring element, work on irregularly sampled data, and can be made more robust to the problems of traditional discrete morphology that stem from the dependence on the sampling grid.

## 2.1 Definitions

A *complete lattice* is the basic structure underlying mathematical morphology.

**Definition 1.** *A complete lattice is a partially ordered set* $(\mathcal{L}, \preceq)$ *where every subset* $X \subset \mathcal{L}$ *has an infimum and a supremum in* $\mathcal{L}$.

Let us define two binary operators $\oplus$ and $\ominus$ on functions $F, G \in \bar{\mathbb{R}}^{\mathbb{R}}$, where $\bar{\mathbb{R}} = \mathbb{R} \cup \{-\infty, \infty\}$ (i.e. one-dimensional grayscale images):

**Definition 2.** *The* dilation *of F by G is defined as*

$$(F \oplus G)(x) = \bigvee_{h \in \mathbb{R}} \big(F(x-h) + G(h)\big),$$

**Definition 3.** *The* erosion *of F by G is defined as*

$$(F \ominus G)(x) = \bigwedge_{h \in \mathbb{R}} \big(F(x+h) - G(h)\big).$$

Unless otherwise specified, we will consider the special case where $G$ is flat, i.e.

$$G(x) = \begin{cases} 0, & \text{if } x \in [a, b] \\ -\infty, & \text{otherwise} \end{cases}. \tag{1}$$

Then the dilation and erosion can be rewritten as

$$(F \oplus G)(x) = \bigvee_{h \in [a,b]} F(x-h), \tag{2}$$

and

$$(F \ominus G)(x) = \bigwedge_{h \in [a,b]} F(x+h), \tag{3}$$

respectively.

## 2.2 Mapping Irregularly Sampled Data Onto Functions over Reals

We define morphology on irregularly sampled data by relating the sampled signals to elements of a complete lattice. Let

$$\mathcal{S} = \mathcal{P}(\mathbb{Z} \times \bar{\mathbb{R}}), \tag{4}$$

be the set of possible sample values, where $\mathcal{P}$ denotes the power set. Then a sampling of a function is an element from the set

$$\mathbb{S} = \left\{ V \in \mathcal{S} \;\middle|\; \text{for all } (x_i, y_i), (x_j, y_j) \in V,\ x_i = x_j \Rightarrow y_i = y_j \right\}. \tag{5}$$

I.e., a sampling is a set of pairs of values where the first element represents the point at which the sample was taken, and the second element represents the value. The sampling is not allowed to take two different values at the same time, i.e., each pair in a sampling corresponds to a value $x$ and its mapping $y$ by some function $f$. We will define a partial order $\preceq$ on $\mathbb{S}$, such that $(\mathbb{S}, \preceq)$ forms a complete lattice.

Since two irregular samplings will not generally be defined at the same points, it is not especially interesting to compare corresponding points to establish the order (most samplings will not be comparable). Instead, in order to compare elements of $\mathbb{S}$, we define the *top*, $T : \mathbb{S} \to \bar{\mathbb{R}}^{\mathbb{R}}$, of a sampled signal $V \in \mathbb{S}$ by

$$T(V)(x) = \begin{cases} f_V(x), & \text{if } x \in [x_{\text{inf}}, x_{\text{sup}}] \\ -\infty, & \text{otherwise} \end{cases} \tag{6}$$

where

$$x_{\text{inf}} = \bigwedge_{x \in X(V)} x, \tag{7}$$

$$x_{\text{sup}} = \bigvee_{x \in X(V)} x, \quad \text{and} \tag{8}$$

$$f_V(x) \text{ is an interpolating function on the samples of } V. \tag{9}$$

Here $X(V) = \{x \mid (x, y) \in V\}$.

Now we may map any irregularly sampled signal onto its corresponding top, which is a function defined everywhere on $\mathbb{R}$. This gives rise to a partial order $\preceq$, namely, for two signals $U$, $V \in \mathbb{S}$

$$U \preceq V \iff T(U) \leq T(V), \tag{10}$$

where $T(U) \leq T(V)$ iff $T(U)(x) \leq T(V)(x)$ for all $x \in \mathbb{R}$. Thus we have imposed a partial order on the irregularly sampled signals. However, this is not enough! In order for $(\mathbb{S}, \preceq)$ to form a complete lattice, every subset $\mathcal{X} \subset \mathbb{S}$ must have an infimum and a supremum in $\mathbb{S}$.

Let us consider the pointwise supremum of the tops of the elements of $\mathcal{X} \subset \mathbb{S}$, i.e., the family of functions $\{T(V_i)\}_{V_i \in \mathcal{X}}$. Clearly, the supremum exists for any such subset, since the top of any element of $\mathbb{S}$ is a function from $\mathbb{R}$ to $\bar{\mathbb{R}}$. However, $\mathcal{X}_V = \bigvee\{T(V_i)\} \notin \mathbb{S}$, since elements of $\mathbb{S}$ are sets of isolated points. Thus, we need to find a set of samples that represents $\mathcal{X}_V$. An element in $\mathbb{S}$ that represents the supremum of $\mathcal{X}$ is, we suggest, a set of samples $V_V$, for which

$$T(V_V) = \mathcal{X}_V. \tag{11}$$

However, in general, such a sampling does not exist! This is clear, since the supremum of two band-limited signals is generally not band-limited, and therefore $\mathcal{X}_V$ cannot be reconstructed from a set of samples with a frequency limited by $\mathbb{Z}$, using some interpolating function $f_V$. However, in the following section we shall see that it is possible to define a kind of top such that, under certain conditions, $V_V$ can be constructed.

Note that two different samplings can give rise to the same top. We therefore define the following equivalence class:

**Definition 4.** *For an element $V \in \mathbb{S}$, its equivalence class $[V]$ is defined as*

$$[V] = \{U \in \mathbb{S} \mid T(U) = T(V)\} \tag{12}$$

## 2.3 Shift Morphology Lattice

In this section we present theory required to construct a top, which may be used to compare irregularly sampled signals. We show that the top can be uniquely defined by a sampling in $\mathbb{S}$, and that using this top with the partial order defined in Eqn. (10) yields a complete lattice $(\mathbb{S}, \preceq)$, which is a step on the way to defining morphological operators on irregularly sampled signals. We call this complete lattice the *shift morphology lattice*, because it will be used to show some properties of operators proposed in this paper, which are computed by duplicating and *shifting* samples.

**Definition 5.** *We define the function $T$ of an irregular signal $V \in \mathbb{S}$ with $n$ samples as follows: Let us assume that the pairs of $V = \{(x_k, y_k)\}_{k\in\{1,2,\dots,n\}}$ are sorted in ascending order on the first element of each pair, then*

$$T(V)(x) = \begin{cases} \min(y_k, y_{k+1}), & \text{if } x_k < x < x_{k+1} \\ y_k, & \text{if } x = x_k \\ -\infty, & \text{if } x < x_{\inf} \text{ or } x > x_{\sup} \end{cases} \tag{13}$$

*Also we define $T(\varnothing) = -\infty$.*

I.e., $T(V)$ is made up of single points and line segments that are either open, half-open, or closed. Under this definition of $T$, and the partial order defined in (10), we shall see that $(\mathbb{S}, \preceq)$ forms a complete lattice.

**Definition 6.** *For a set $A$, $\mathbb{1}_A$ is the indicator function:*

$$\mathbb{1}_A(x) = \begin{cases} 1, & \text{if } x \in A \\ 0, & \text{if } x \notin A \end{cases} \tag{14}$$

**Definition 7.** *The open interval, $\{x \in \mathbb{R} \mid a < x < b\}$ is denoted*

$$]a, b[ \tag{15}$$

**Lemma 1.** *For any $V \in \mathbb{S}$, its top $T(V)$ can be written as an infinite series of coefficients $\alpha_i, \beta_i \in \bar{\mathbb{R}}$, and indicator functions*

$$[T(V)](x) = \sum_{i=-\infty}^{\infty} \alpha_i \mathbb{1}_{\{i\}}(x) + \beta_i \mathbb{1}_{]i,i+1[}(x) \tag{16}$$

**Proof.** Assume, without loss of generality, that $V$ is sorted in ascending order on the first element of each sample $(x, y) \in V$. For $i \in \mathbb{Z}$, choose

$$\alpha_i = \begin{cases} y, & \text{if } (i, y) \in V \\ -\infty, & \text{if } i < x_{\inf} \vee i > x_{\sup} \\ \min\{y^-, y^+\} & \text{otherwise} \end{cases} \tag{17}$$

$$\beta_i = \min\{\alpha_i, \alpha_{i+1}\}, \tag{18}$$

where $x_{\inf}$ and $x_{\sup}$ are defined as in Eqn. 7 and 8, and $y^-$ and $y^+$ are the values at positions $x^-$ and $x^+$, where

$$x^- = \max\{x \mid (x, y) \in V \wedge x < i\} \tag{19}$$

$$x^+ = \min\{x \mid (x, y) \in V \wedge x > i\} \tag{20}$$

i.e., $(x^-, y^-), (x^+, y^+) \in V$ are the samples immediately to the left and to the right of $(i, y)$ respectively. Note that $x^-$ does not exist if $i \leq x_{\inf}$, however $\alpha_i$ is still well defined in such cases, since one of the top two conditions of (17) will apply. Similarly, if $i \geq x_{\sup}$, $x^+$ does not exist, but $\alpha_i$ is still well defined. If the signal $V$ is infinite, it may not admit a supremum and/or infimum in $\mathbb{Z}$, however, one may easily extend the domain with $-\infty$ and $\infty$ to address this issue.

By the definition of $\mathbb{S}$, $y$, $y^+$, and $y^-$ are uniquely defined for any given $i$. The series

$$f(x) = \sum_{i=-\infty}^{\infty} \alpha_i \mathbb{1}_{\{i\}}(x) + \beta_i \mathbb{1}_{]i,i+1[}(x) \tag{21}$$

is a function of $x$. For any element $(x, y) \in V$, we have $f(x) = \alpha_x = y$. Similarly, for any consecutive pair $(x_k, y_k), (x_{k+1}, y_{k+1}) \in V$, for any $x \in ]x_k, x_{k+1}[$, $f(x) = \min\{y_k, y_{k+1}\}$, since either $f(x) = \alpha_j$, or $f(x) = \beta_j$, for

some $j \in \mathbb{Z}$. Finally, if $x < x_{\text{inf}}$, or $x > x_{\text{sup}}$, $f(x) = -\infty$. Thus,

$$f(x) = \begin{cases} \min(y_k, y_{k+1}), & \text{if } x_k < x < x_{k+1} \\ y_k, & \text{if } x = x_k \\ -\infty, & \text{if } x < x_{\text{inf}} \text{ or } x > x_{\text{sup}} \end{cases} = T(V)(x) \tag{22}$$

□

**Definition 8.** *We define $T(\mathcal{X})$ as the set containing the tops of all the signals in $\mathcal{X}$, i.e.,*

$$T(\mathcal{X}) = \{T(V) \mid V \in \mathcal{X}\} \tag{23}$$

**Lemma 2.** *For a family of sampled signals $\mathcal{X} \subset \mathbb{S}$, the set of tops $T(\mathcal{X})$ has a supremum $\bigvee T(\mathcal{X})$, which is uniquely defined by a set of constants $\mathcal{A}$, where*

$$\mathcal{A} = \{\alpha_i\}_{i\in\mathbb{Z}} = \left\{ \bigvee_{V\in\mathcal{X}} \alpha_i^V \right\}_{i\in\mathbb{Z}} \tag{24}$$

*Here the $\alpha_i^V$ are the α-coefficients from the tops of $\mathcal{X}$, as in Equation (16).*

**Proof.** For any point $x \in \mathbb{R}$, and any $V \in \mathcal{X}$, by Lemma 1, we have that

$$T(V)(x) = \sum_{i=-\infty}^{\infty} \alpha_i^V \mathbb{1}_{\{i\}}(x) + \beta_i^V \mathbb{1}_{]i,i+1[}(x) = \begin{cases} \alpha_x^V, & \text{if } x \in \mathbb{Z} \\ \beta_{\lfloor x \rfloor}^V, & \text{if } x \notin \mathbb{Z} \end{cases}. \tag{25}$$

Thus, the pointwise supremum of $T(\mathcal{X})$ is

$$\bigvee T(\mathcal{X})(x) = \bigvee_{V\in\mathcal{X}} T(V)(x) = \begin{cases} \bigvee \alpha_x^V, & \text{if } x \in \mathbb{Z} \\ \bigvee \beta_{\lfloor x \rfloor}^V, & \text{if } x \notin \mathbb{Z}. \end{cases} \tag{26}$$

Since $\beta_i^V = \min\{\alpha_i^V, \alpha_{i+1}^V\}$, we have

$$\bigvee \beta_i^V = \bigvee \min\{\alpha_i^V, \alpha_{i+1}^V\} = \min\{\bigvee \alpha_i^V, \bigvee \alpha_{i+1}^V\}, \tag{27}$$

so $\beta_i^V$ is a function of $\bigvee \alpha_i^V$ and $\bigvee \alpha_{i+1}^V$. Therefore, the supremum over $V \in \mathcal{X}$

$$\bigvee T(\mathcal{X})(x) = \begin{cases} \bigvee \alpha_x^V, & \text{if } x \in \mathbb{Z} \\ \min\{\bigvee \alpha_{\lfloor x \rfloor}^V, \bigvee \alpha_{\lfloor x \rfloor + 1}^V\}, & \text{if } x \notin \mathbb{Z}, \end{cases} \tag{28}$$

only depends on $\mathcal{A}$.

□

**Theorem 1.** *For a subset $\mathcal{X} \subset \mathbb{S}$, there exists some element $V_\vee \in \mathbb{S}$, such that*

$$\bigvee_{V\in\mathcal{X}} T(V) = T(V_\vee) \tag{29}$$

**Proof.** By Lemma 2 there exists a set of constants $\mathcal{A}$, which defines $\bigvee_{V\in\mathcal{X}} T(V)$, namely:

$$\mathcal{A} = \{\alpha_i\}_{i\in\mathbb{Z}} = \left\{ \bigvee_{V\in\mathcal{X}} \alpha_i^V \right\}_{i\in\mathbb{Z}} \tag{30}$$

let us consider the set of pairs

$$\mathcal{A}^S = \{(i, \alpha_i) \mid i \in \mathbb{Z}, \alpha_i \in \mathcal{A}\} \tag{31}$$

We will show that $\mathcal{A}^S$ is $V_\vee$. Clearly, $\mathcal{A}^S \in \mathbb{S}$, and

$$T(\mathcal{A}^S)(x) = \begin{cases} \min\{\alpha_i, \alpha_{i+1}\}, & \text{if } i < x < i+1 \\ \alpha_i, & \text{if } x = i \\ -\infty, & \text{if } x < x_{\inf} \text{ or } x > x_{\sup} \end{cases} \tag{32}$$

$$= \begin{cases} \min\{\alpha_i, \alpha_{i+1}\}, & \text{if } i < x < i+1 \\ \alpha_i, & \text{if } x = i \end{cases} \tag{33}$$

$$\text{(By (30))} = \begin{cases} \min\{\bigvee \alpha_i^V, \bigvee \alpha_{i+1}^V\}, & \text{if } i < x < i+1 \\ \bigvee \alpha_i^V, & \text{if } x = i \end{cases} \tag{34}$$

$$\text{(By proof of Lemma 2)} = \bigvee_{V \in \mathfrak{X}} T(V)(x) \tag{35}$$

Thus, $V_\vee = \mathcal{A}^S$ satisfies Equation (29). Note that there may be other samplings that also satisfy the equation, however, by definition, these belong to the same equivalence class (see Def. 4).

□

**Definition 9.** *For a subset $\mathfrak{X} \subset \mathbb{S}$, its supremum is defined as*

$$\bigvee \mathfrak{X} = V_\vee, \tag{36}$$

*where $T(V_\vee) = \bigvee_{V \in \mathfrak{X}} T(V)$.*

By a similar procedure we can show that

**Theorem 2.** *For a subset $\mathfrak{X} \subset \mathbb{S}$, there exists some element $V_\wedge \in \mathbb{S}$, such that*

$$\bigwedge_{V \in \mathfrak{X}} T(V) = T(V_\wedge) \tag{37}$$

**Proof.** The proof follows the proof of Theorem 1 except for appropriate substitutions.

□

This leads to the definition of the infimum:

**Definition 10.** *For a subset $\mathfrak{X} \subset \mathbb{S}$, its infimum is defined as*

$$\bigwedge \mathfrak{X} = V_\wedge, \tag{38}$$

*where $T(V_\wedge) = \bigwedge_{V \in \mathfrak{X}} T(V)$.*

By theorems 1 and 2, the supremum and infimum exist. Note that the supremum and infimum of a signal is not necessarily unique, in the sense that they may be sampled in different ways. However, for any two suprema, $V_\vee^1$, and $V_\vee^2$ of a signal $\mathfrak{X}$, they belong to the same equivalence class, and are equivalent under the partial order defined in (10). This, of course, also goes for the infimum.

**Corollary 1.** $(\mathbb{S}, \preceq)$ *forms a complete lattice.*

**Proof.** Follows trivially from theorems 1 and 2, and the partial ordering of Equation (10).

□

The sampling $V_\vee$ given in Equation (31) is just one possible sampling (in fact a regular sampling), which generally contains more points than necessary. Indeed, for any three consequtive samples with the same value, one of them is redundant. Let $|X|$ denote the cardinality of $X$. The smallest set of samples that can represent the supremum is the set of samples $V_\vee^m \in [V_\vee]$, such that $|V_\vee^m| \leq |U|$, for all $U \in [V_\vee]$. There may be many such smallest sets.

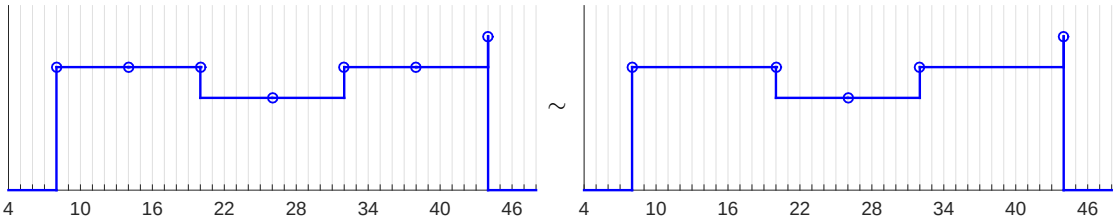


**Figure 4:** Two sampled signals (blue circles), which are equivalent, since they have the same tops (blue lines).

Also note that one may freely choose the interpolating function in the definition of the top (13), however, choosing some other function may mean that a complete lattice cannot be defined.

Finally, it is worth mentioning that even though the samples are elements of $\mathbb{S}$, thus restricting the sampling time to integer values, the minimal sampling distance can be chosen arbitrarily close, as long as the minimal distance is fixed, by changing the scale (see Thm. 4).

## 2.4 Shift Morphology and Dilations, Erosions, Openings, and Closings

Above we defined a complete lattice on irregularly sampled signals. In this section we shall define some important operators of mathematical morphology on such samplings; namely: Dilations, erosions, openings, and closings.

### 2.4.1 Shift Morphology

We define the dilation with a flat structuring element of an irregularly sampled signal via the traditional dilation of the top function, i.e.

**Definition 11.** *For an irregularly sampled signal $V \in \mathbb{S}$, and a structuring element $G \in \bar{\mathbb{R}}^{\mathbb{Z}}$, the irregular dilation, $\oplus_I$, is defined as:*

$$V \oplus_I G = V_{\text{dil}} \tag{39}$$

*where*

$$V_{\text{dil}} = \{(x, [T(V) \oplus G](x)) \mid x \in \mathbb{Z}\} \tag{40}$$

*where $\oplus$ is the continuous dilation of Definition 2.*

Note that $V_{\text{dil}}$ is a member of an equivalence class, $[V_{\text{dil}}]$, which may contain many other equivalent samplings (see Fig. 4).

It is clear that this is a dilation. First note that by Def. 9:

$$T\left(\bigvee_{V \in \mathfrak{X}} V\right) = T(V_\vee) = \bigvee_{V \in \mathfrak{X}} T(V) \tag{41}$$

Then, we have that:

$$T\left(\bigvee (V \oplus_I G)\right) = T\left(\bigvee \{(x, [T(V) \oplus G](x)) \mid x \in \mathbb{Z}\}\right) \tag{42}$$

$$\text{(by Eqn. 41)} = \bigvee T\left(\{(x, [T(V) \oplus G](x)) \mid x \in \mathbb{Z}\}\right) \tag{43}$$

$$\text{(by proof of Theorem 1)} = T\left(\left\{\left(x, \bigvee \left[T(V) \oplus G\right](x)\right) \mid x \in \mathbb{Z}\right\}\right) \tag{44}$$

$$\text{(since } \oplus \text{ is the continuous dilation)} = T\left(\left\{\left(x, \left[\left(\bigvee T(V)\right) \oplus G\right](x)\right) \mid x \in \mathbb{Z}\right\}\right) \tag{45}$$

$$\text{(by Def. 11)} = T\left(\left(\bigvee V\right) \oplus_I G\right) \tag{46}$$

I.e., the dilation, $\oplus_I$, distributes over the supremum. However, is there an efficient way to compute this operation, i.e., to find a member of the equivalence class? We shall see that one may perform the irregular dilation without constructing the top, or explicitly performing a dilation of a function, or even explicitly rescaling the signal, but first let us consider what happens when this dilation is applied to *regularly sampled* signals:

**Definition 12.** *For a regularly sampled signal $f : \mathbb{Z} \to \bar{\mathbb{R}}$, its regular, discrete dilation with a flat structuring element $G$, which is 0 for values in $[a, b] \subset \mathbb{Z}$ and $-\infty$ otherwise is defined as*

$$f \oplus_R G = \bigvee_{h \in [a,b]} f(x - h) \tag{47}$$

**Theorem 3.** *For any $V \in \mathbb{S}$, such that for all $x \in \mathbb{Z}$ there is some $y \in \bar{\mathbb{R}}$, such that $(x, y) \in V$ and for all $(x, y) \in V$, $x \in \mathbb{Z}$ and $y \in \bar{\mathbb{R}}$, the following equality holds:*

$$V \oplus_I G = V \oplus_R G,$$

*where $\oplus_I$ is the irregular dilation, $\oplus_R$, is the regular, discrete dilation, $G$ is a structuring element defined by $[a, b]$, where $a, b \in \mathbb{Z}$, $a < b$, and equality is given by the partial order defined in* (10).

**Proof.** We only need to consider $x \in \mathbb{Z}$, for which we have that, by Definition 11

$$T(V \oplus_I G)(x) = (T(V) \oplus G)(x) \tag{48}$$

$$\text{(By (2))} = \bigvee_{h \in [a,b]} \left(T(V)(x - h)\right) \tag{49}$$

$$\text{(By Lemma 1)} = \bigvee_{h \in [a,b]} \sum_i \alpha_i \mathbb{1}_{\{i\}}(x - h) + \min\{\alpha_i, \alpha_{i+1}\} \mathbb{1}_{]i,i+1[}(x - h) \tag{50}$$

$$\text{(Since } \alpha_i \geq \min(\alpha_i, \alpha_{i+1})\text{)} = \bigvee_{h \in [a,b]} \sum_i \alpha_i \mathbb{1}_{\{i\}}(x - h) \tag{51}$$

$$\text{(Since } x \in \mathbb{Z}\text{, and } a, b \in \mathbb{Z}\text{)} = \bigvee_{h \in \{a, a+1, \ldots, b-1, b\}} \sum_i \alpha_i \mathbb{1}_{\{i\}}(x - h) \tag{52}$$

$$= \bigvee_{h \in \{a, a+1, \ldots, b-1, b\}} \alpha_{x-h} \tag{53}$$

$$\text{(By (17))} = \bigvee_{h \in \{a, a+1, \ldots, b-1, b\}} y_{x-h} \tag{54}$$

$$\text{(By Def. 12)} = T(V \oplus_R G)(x) \tag{55}$$

Where $y_i \in \bar{\mathbb{R}}$ is the value of the top at $x_i \in \mathbb{Z}$.

□

Thus, applying the irregular version of dilation to a regularly sampled signal, where the distance between samples is 1, yields the same result as applying the regular dilation to the same sampled signal. In other words, in the special case where the signal is regularly sampled and the SE depends on this sampling grid, the irregular dilation is equivalent to the regular dilation.

We can now define the erosion by duality.

$$V \ominus G = -((-V) \oplus \check{G}) \tag{56}$$

Since we have the dilation and erosion, it is now easy to define openings and closings by composition. Clearly these yield samplings that are elements of $\mathbb{S}$, since the result of the irregular dilation, as well as the irregular erosion, is in $\mathbb{S}$, as long as the original sampling is in $\mathbb{S}$.

In the following theorem, we show that a family of complete lattices can be constructed, which may be used to show that irregular dilations may be applied in a more general case where the sample positions are not restricted to integer coordinates. This is done by a change of coordinates so that we can represent samples at locations that are integer multiples of some $d_{\min} \in \mathbb{R}$. This $d_{\min}$ can be though of as the distance between grid points in a regular sampling grid.

**Theorem 4.** *Choosing* $0 < d_{\min} \in \mathbb{R}$, *and* $m \in \mathbb{Z}^+$, *let* $\mathcal{S}_x^{d_{\min}} = \{id_{\min} \mid i \in \mathbb{Z}\}$, $\mathcal{S}^{d_{\min}} = \mathcal{P}(\mathcal{S}_x^{d_{\min}} \times \bar{\mathbb{R}})$, *and*

$$\mathbb{S}^{d_{\min}} = \left\{ V \in \mathcal{S}^{d_{\min}} \;\middle|\; \text{for all } (x_i, y_i), (x_j, y_j) \in V,\ x_i = x_j \Rightarrow y_i = y_j \right\} \tag{57}$$

*Then,* $(\mathbb{S}^{d_{\min}}, \preceq)$, *where* $\preceq$ *is as in Eqn. (10) forms a complete lattice, and for any element* $V \in \mathbb{S}^{d_{\min}}$, *the dilation*

$$V \oplus G = V_{\text{dil}}^{\mathbb{S}^{d_{\min}}} \tag{58}$$

*where G is a structuring element of length* $md_{\min}$, *is an element* $V_{\text{dil}}^{\mathbb{S}^{d_{\min}}} \in \mathbb{S}^{d_{\min}}$

**Proof.** There is a mapping between $\mathbb{S}^{d_{\min}}$ and $\mathbb{S}$ for a given $d_{\min} > 0$. Namely, for an element

$$V^{d_{\min}} = \{(x_1, y_1), (x_2, y_2), \dots\} \in \mathbb{S}^{d_{\min}} \tag{59}$$

$$V^{d_{\min}} \mapsto \{(x_1/d_{\min}, y_1), (x_2/d_{\min}, y_2), \dots\} \in \mathbb{S} \tag{60}$$

In fact, this is a bijection, since we can easily invert the mapping by multiplying with $d_{\min}$. Similarly, since the length of the structuring element $G$ is assumed to be $md_{\min}$, the mapping gives us a structuring element $G'$ of length $m$, and since $m \in \mathbb{Z}^+$, the dilation exists as an element in $\mathbb{S}$. So $\mathbb{S}$ and $\mathbb{S}^{d_{\min}}$ are isomorphic. Thus, $\mathbb{S}^{d_{\min}}$ forms a complete lattice, and we can compute the dilation of $V \oplus G$ in $\mathbb{S}^{d_{\min}}$, by computing the corresponding dilation in $\mathbb{S}$.

□

### 2.4.2 Computing the Irregular Dilation

We take inspiration from the traditional definition of dilation for a grayscale function. Figure 5 shows an example of a one-dimensional dilation of a continuous signal using a flat structuring element. Notice that the dilation is formed by sliding the structuring element (i.e. the line segment) along the top of the signal, the dilated signal is traced by the origin of the SE. Another way of looking at it is to consider the line segment as its *origin* slides along the top of the signal, then its end points trace out the dilation. This interpretation naturally gives rise to a type of dilation on irregular samples. The idea can be broken down into four steps:

1. For each sample, translate the SE such that its origin coincides with the sample.
2. Make two copies of the sample.
3. Shift the two copies to the end points of the SE.
4. Supress samples that could be under the SE when it is placed at a sample of greater value.

Figure 6 shows an illustration of this procedure. The suppression of a sample created in step 2 is performed by shifting the sample in question towards its parent, until the sample is no longer in the shadow of a SE as

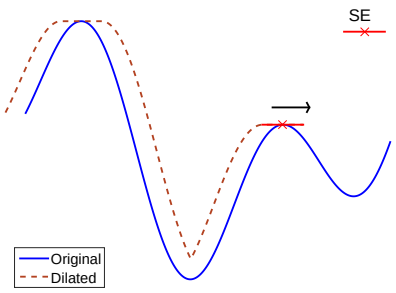


**Figure 5:** Dilation (dashed brown) of a one-dimensional continuous signal (blue) with a flat structuring element (red). The origin of the SE is marked with an 'x.'

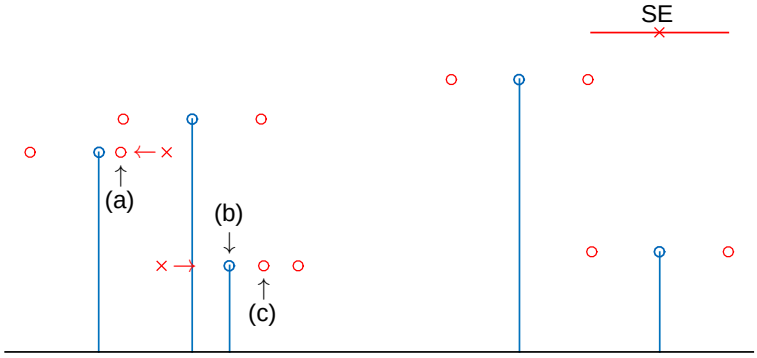


**Figure 6:** Illustration of the dilation (red + blue, except (b)) of an irregularly sampled signal (blue) via duplicating and shifting samples. Arrow (a) indicates a duplicated sample that was moved left (from the red x to its right) because it was suppressed by the sample above it. Arrow (b) indicates an original sample that is removed, since it is suppressed by the duplicated sample above it. Arrow (c) indicates a duplicated sample that was shifted right because of suppression (from the red x to its left). Samples that are shifted because of suppression are moved in the direction of the sample that spawned them until they are outside the suppressing area by some margin, $\varepsilon$.

described in step 4. An additional shift by $\varepsilon$ length units is performed, so that the sampled function does not take two different values at the same position. Supression of input samples is simply done by deletion.

This process applied to any element $V \in \mathbb{S}$, we will see, gives an (irregular) sampling that reconstructs the dilation of the top of the signal as defined in previous sections, under certain conditions. Therefore this yields the irregular dilation of $V$. Thus, as shown in Theorem 3, the result of applying these steps to a regularly sampled signal is equivalent to applying the traditional dilation to the same set of samples. However, nothing prevents us from applying these steps to an *irregularly* sampled signal instead, yielding a dilation (under certain restrictions, as discussed in Section 2.4.1).

The pseudo-code for an implementation of this algorithm can be seen in Alg. 1. First we sort the input nodes in descending order (based on their value), since when considering the suppression of some sample, $(x, y)$, we only need to consider samples $(x', y')$, such that $y' > y$. This is similar to the approach in a paper by Dokládal and Dokládalová [8], which presents a way of computing regular 1D-dilations by ignoring values, that will not affect the dilation, in a similar way. We then check if a duplicated sample $i^-$ should be suppressed (i.e., if a neighboring node at a higher value is close enough that the SE causes a suppression). We do the same for the duplicated sample $i^+$. If the duplicated samples switch order, so that $i^- > i^+$ after shifting, we discard the duplicated samples (because there is no available position they can occupy without still requiring suppression). Finally, we check to see if the input sample $i$, which spawned $i^-$ and $i^+$ needs to be suppressed (in which case it is deleted). This happens when one of the duplicated samples $i^-$ or $i^+$ has been shifted past the parent sample $i$.

If a self-balancing binary search tree [9] is used to store the list of preceding nodes NODES$^-$, the complexity of the algorithm will be $\mathcal{O}(N \log N)$, where $N$ is the number of samples in the input.

**Algorithm 1:** Duplicate-and-shift dilation pseudocode.

**Data:** A list of input samples, NODES, which contains positions and values for each sample. The left, and right edges, $SE^-$, and $SE^+$, of the SE as offsets from the origin. A scalar, $\varepsilon \in \mathbb{R}^+$, which depends on the distance between samples in the input, and is used to prevent the output taking two different values at the same position.

**Result:** A list of output samples DNODES which contains positions and values for each sample in the dilated signal.

```
1  Function Dilate–Irregular (NODES, SE⁻, SE⁺)
2      let DNODES be an empty array
3      sort NODES according to y-value in descending order
4      for each node i ∈ NODES do
5          let i⁻ and i⁺ be duplicates of i
6          let pos(i⁻) = pos(i) + SE⁻
7          let pos(i⁺) = pos(i) + SE⁺
8          let NODES⁻ be the list of nodes that precede i (thus, the y-values of nodes in this list are greater
             than the y-value of i)
9          let j⁻ be the nearest neighbor of i in NODES⁻, s.t. pos(j⁻) < pos(i)
10         let j⁺ be the nearest neighbor of i in NODES⁻, s.t. pos(j⁺) > pos(i)
11         //If j⁻ does not exist, let pos(j⁻) = −∞
12         //If j⁺ does not exist, let pos(j⁺) = +∞
13         if pos(i⁻) ≤ pos(j⁻) + SE⁺ then
14             pos(i⁻) = pos(j⁻) + SE⁺ + ε
15         if pos(i⁺) ≥ pos(j⁺) + SE⁻ then
16             pos(i⁺) = pos(j⁺) + SE⁻ − ε
17         if pos(i⁻) ≤ pos(i⁺) then
18             if ∄n ∈ DNODES : pos(i⁻) = pos(n) then
19                 insert i⁻ into DNODES
20             if ∄n ∈ DNODES : pos(i⁺) = pos(n) then
21                 insert i⁺ into DNODES
22             if pos(i⁻) < pos(i) < pos(i⁺) then
23                 insert i into DNODES
24         else
25             drop nodes i⁻, i, and i⁺
26     return DNODES
```

The implementation of erosion, opening, and closing is trivial (using duality and composition). Note however, that in general, for an irregularly sampled signal $V$, the top of its complement $T(-V)$ is not equal to the complement of its top, $-T(V)$. Thus, applying the algorithm to the complement of the irregularly sampled signal, will not generally yield an actual erosion (and therefore the opening and closing by composition will not be actual openings or closings either). In the special case where the signal is sampled regularly (from $-\infty$ to $\infty$) however, the difference between the complement of the top of $V$ and the top of the complement of $V$ does not affect the values at the samples in the erosion (i.e., the algorithm yields an actual erosion). In the following experiments, we will ignore this issue and compute the erosion naively by applying the algorithm to $-V$ and taking the complement of the output. We shall see that, empirically, the algorithm still yields good approximations.

Figure 7 shows a toy example where the proposed 1D-opening is applied to an irregulary sampled 1D-signal extracted from a sampled rock pile using SEs of different sizes. As the size of the SE increases, larger plateaus are created, which require fewer samples. The opened signal may be interpolated back onto the orig-

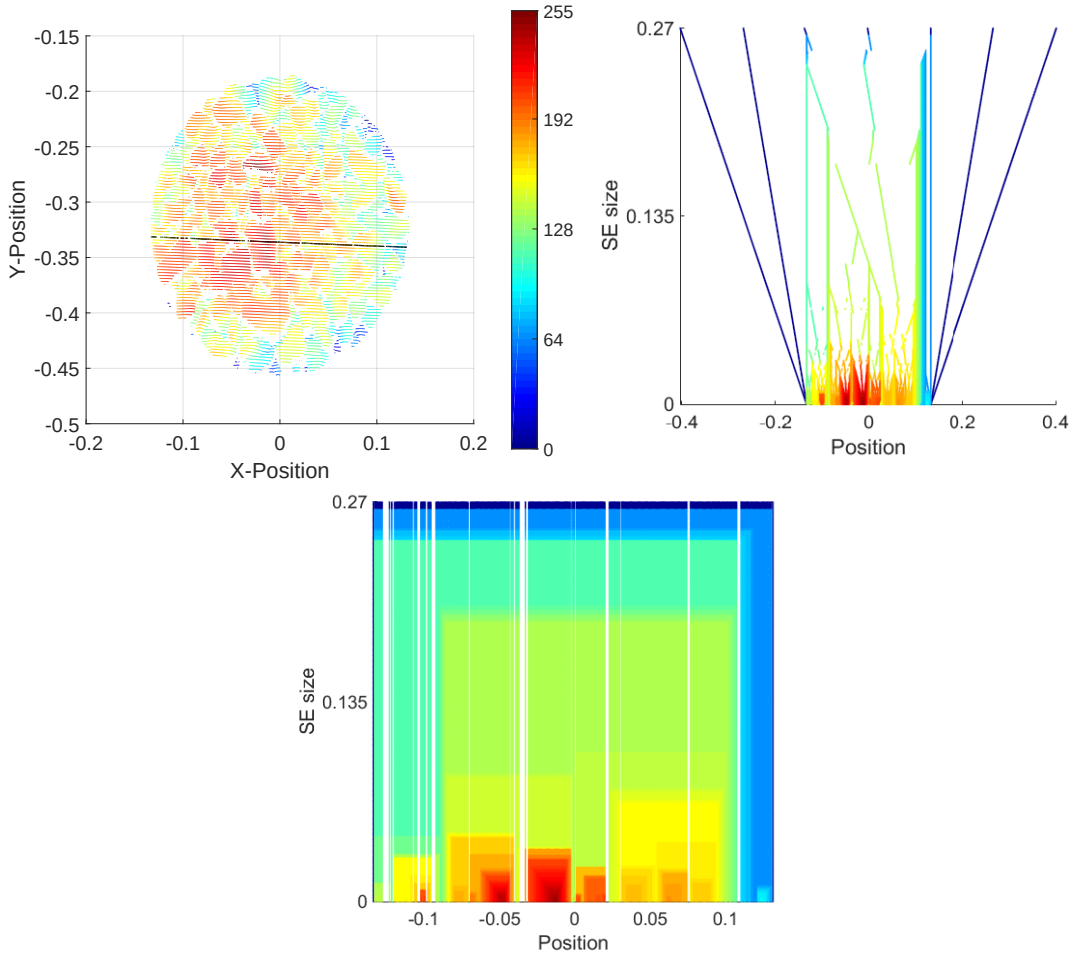


**Figure 7:** An example where the proposed 1D-opening is applied to an irregularly sampled signal extracted from a sampled rock pile. Top row: On the left, the sampled rock pile. The black samples indicate the extracted 1D-signal. On the right, 1D-openings of the extracted signal with varying SE sizes (from 0 length units at the bottom, to 0.27 at the top). Each horizontal slice represents a single 1D-opening. The colormap indicates the value of the samples. Note that two samples of value 0 were added to the extracted signal at each end, to enforce border conditions. As the size of the SE increases, bigger plateaus are created, therefore the signal requires fewer samples (the number of samples is decimated from 340 in the input signal, to 12 in the opening for the largest SE). The bottom figure shows the result of interpolating the opened signal back onto the input positions.

inal sample positions if one desires to keep the number of samples, as well as the sample positions, constant (using, for example, linear interpolation, as in this example).

We shall prove that Alg. 1 applied to an element $V \in \mathbb{S}$, yields a new element, which is equivalent to the dilation of $V$, under certain restrictions. First we need the following lemma:

**Lemma 3.** *A sampled signal $V \in \mathbb{S}$ has a piecewise constant top $T(V)$. A signal $V'$, which contains a sample at each endpoint of every plateau in $T(V)$, at least one sample on each plateau (except the plateau beginning at $-\infty$, and the one ending at $+\infty$), and no samples which are not taken from $T(V)$, belongs to the same equivalence class as $V$, i.e.,*

$$T(V) = T(V') \tag{61}$$

**Proof:** It follows immediately from Lemma 1 that $T(V)$ is piecewise constant. By endpoints of a plateau, we mean those points $p_i$ where the left and right limits do not agree, i.e.,

$$\lim_{x \to p_i^+} T(V)(x) \neq \lim_{x \to p_i^-} T(V)(x) \tag{62}$$

Assume that the endpoints are ordered according to their position in ascending order. If the plateau is of length 0, then the plateau will be captured by the endpoint. Otherwise:

If the plateau contains both endpoints, i.e., if the endpoints $p_i$, and $p_{i+1}$ of a plateau take the value $T(V)(x)$ where $p_i < x < p_{i+1}$, then a signal $V'$ sampling $T(V)$, which samples $p_i$, and $p_{i+1}$ will have a top $T(V')$ which is equal to $T(V)$ between $p_i$ and $p_{i+1}$. This follows from the definition of the top (Def. 5), since $T(V)(p_i) = T(V')(p_i)$, $T(V)(p_{i+1}) = T(V')(p_{i+1})$, and the minimum value of samples between $p_i$, and $p_{i+1}$ is necessarily the same as the value of $p_i$, and $p_{i+1}$, since they are the endpoints of a constant plateau.

If the plateau contains one of the endpoints $p_i$, but not the other endpoint $p_{i+1}$, then it holds for the top of the original signal $V$, that $T(V)(p_i) < T(V)(p_{i+1})$ (because of the minimum). Therefore, the top of $T(V')$ will take the value of $T(V)(p_i)$ for all $x$, s.t. $p_i < x < p_{i+1}$. Since $T(V)(x)$ is constant for $p_i < x < p_{i+1}$, and $T(V)(x)$ is the minimal value of the two samples $p_i$ and $p_{i+1}$, $T(V)(x) = T(V')(x)$, for $p_i \leq x \leq p_{i+1}$. The same argument holds if $p_{i+1}$ is contained in the plateau, but not $p_i$.

Finally, a plateau may contain none of its endpoints. In this case, the lemma requires that there is at least one sample at $p$ between $p_i$, and $p_{i+1}$ (since each plateau must have at least one sample). If a plateau contains none of its endpoints, this means that $T(V)(p) < T(V)(p_i)$, and $T(V)(p) < T(V)(p_{i+1})$, since the value between the endpoints is the minimum of the value at the endpoints and the value at the plateau. Therefore, $T(V')(x) = T(V)(x)$ for $p_i < x < p_{i+1}$.

Thus, for all possibilities (i.e., the plateau contains all endpoints, one endpoint, or no endpoints), the value of $T(V')$ between two endpoints is equal to the value of $T(V)$ between the same points. Since each endpoint is sampled, the value between all endpoints is the same for both $T(V)$ and $T(V')$. Obviously, the value at the endpoints is the same for both tops, therefore, $T(V) = T(V')$ everywhere. Therefore, it is sufficient for a signal to be sampled at the endpoints of the top and once for every plateau to be equivalent to that top. □

We will now go on to show that, for $d_{\min} = \varepsilon = 1$, and input signal $V \in \mathbb{S}$, Alg. 1 yields an element $V_o \in \mathbb{S}$, such that, for a SE $G$, which is 0 for values in $G_0 = [a, b] \subset \mathbb{R}$, where $a < 0 < b$, and $a, b \in \mathbb{Z}$ and $-\infty$ otherwise, and for element $V_{\text{dil}} \in \mathbb{S}$, where $V_{\text{dil}} = V \oplus_I G$, we have $V_o \sim V_{\text{dil}}$ (i.e. $V_o \in [V_{\text{dil}}]$).

It is easily shown that the algorithm yields an output in $\mathbb{S}$, simply note that the position of nodes start at integer values and any nodes in the output are placed at integer valued distances from the input nodes, thus the output contains nodes solely at integer positions. Moreover, there will never be two nodes $(x, y)$, and $(x, y')$ in the output, such that $y \neq y'$, since when inserting the second node at position $x$, there would have been a previously inserted node in DNODES with the same position, but with a higher value, which would prohibit inserting the other node at that position (see lines 18, 20, and 22 in Alg. 1). Therefore, the output of Alg. 1 contains nodes $(x_i, y_i)$, such that $x_i \in \mathbb{Z}$, $y_i \in \bar{\mathbb{R}}$, and for any pair of nodes $(x_i, y_i)$, $(x_j, y_j)$ in the output $x_i = x_j \Rightarrow y_i = y_j$. Thus the output is an element of $\mathbb{S}$.

To show that the algorithm yields a sampled signal

$$V_o \sim V_{\text{dil}} = V \oplus_I G, \tag{63}$$

for an input $V \in \mathbb{S}$, consider the dilation of the top of $V$ at a sample $v$. Either $v$ gives rise to part of a plateau in the dilation, or $v$ (and the part of a plateau that it would generate) is subsumed by a plateau above it (see Fig. 8). Note that the algorithm presented in Alg. 1 places samples at the extreme ends of the SE placed at $v$, unless they are subsumed by a plateau above it. Since the endpoints of every plateau depend on the endpoints of the SE placed at a sample, we can be sure that all endpoints of plateaus contained in the dilation will be sampled, thus fulfilling the first condition of Lemma 3.

Moreover, if the endpoints of the SE are covered by a segment above it (lines 13-16), the plateau is still sampled, as long as there is $2\varepsilon$ space between the nearest endpoint to the left and the nearest endpoint to the right. Since $\varepsilon = 1$ and the input signal is in $\mathbb{S}$ (i.e., the distance between samples is at least 1), this means

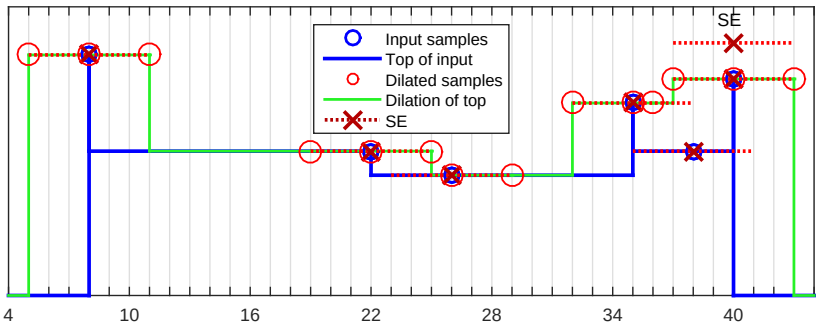


**Figure 8:** Illustration of the steps of the algorithm. The blue solid line illustrates the top of the input samples (blue circles behind the red crosses). The green line illustrates the continuous dilation of the top. Note that the vertical lines are only there for illustration purposes, the actual dilation has a discontinuity at these points, where the higher value is part of the signal, while the lower is not. The algorithm places the SE (illustrated in the top right) at each input sample and creates two new samples at its endpoints and one at the origin. The endpoints (red circles) are then moved so that they are not placed below a previously placed segment. Note that every endpoint of the plateaus of the dilated top must necessarily correspond to some endpoint of the SE placed on top of an input sample. Not every sample in the output of the algorithm will be an endpoint of a plateau in the top (see, for example, the fourth sample in red from the left), but every endpoint of a plateau in the top will have a sample. Furthermore, note that each plateau in the top of the dilation will have a sample, unless the plateau is too small (see Fig. 9), so that the plateau does not stretch over an interval containing an integer. In such cases, the dilation will not contain a sample for this plateau either.

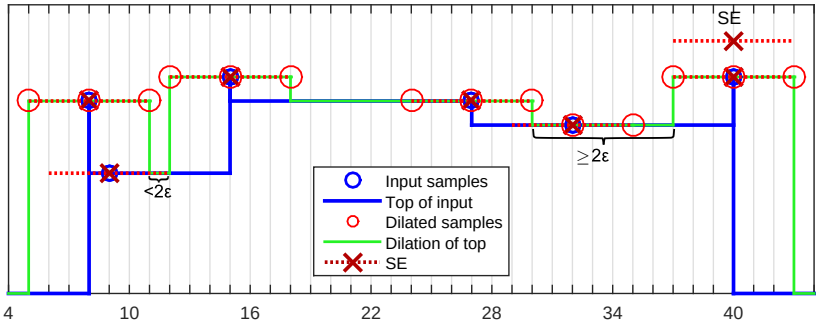


**Figure 9:** Illustration of the steps of the algorithm. The blue solid line illustrates the top of the input samples (blue blobs behind the red crosses). The green line illustrates the continuous dilation of the top. The algorithm places the SE at each input sample and creates two new samples at its endpoints and one at the origin (red circles). In this example, since there is a plateau of size $< 2\varepsilon$, this plateau will not be sampled. Therefore, it cannot be reconstructed by the top of the output of the algorithm. This, however, is not a problem, since the dilation does not capture this plateau either, because the dilation is defined as the top of samples at integer locations, and there is no integer in the interval, since the endpoints are placed at integer locations, and the distance between them is less than $2\varepsilon = 2$.

that any plateau that is defined over a segment containing an integer will be sampled (see Fig. 9). Since the dilation of $V$, i.e., $V_{\text{dil}}$, is the continuous dilation of $T(V)$ sampled at each integer position, the plateaus of the top $T(V_{\text{dil}})$ must stretch over intervals containing some integer. We now have that each plateau in the top of the dilation is sampled at least once in $V_o$, all the endpoints of plateaus are sampled, and there are no samples outside of plateaus. Therefore, by Lemma 3, the output of the algorithm, $V_o$, is equivalent to $V \oplus_I G$.

Note that, by Theorem 4, we can instead consider signals of $\mathbb{S}^{d_{\min}}$, thus allowing for structuring elements $G$ of arbitrary sizes. However, also note that the algorithm itself is not necessarily bound by any restrictions on $G$, $\varepsilon$, or sampling positions (although $\varepsilon$ should normally be chosen less than or equal to $d_{\min}$). In fact, in the following section we shall see that we can achieve better results by breaking these constraints (along with using an interpolation that creates samples not lying on the dilation of the top in Definition 5), while

still being guided by them, although the result of applying the algorithm is no longer necessarily a dilation, strictly speaking.

# 3 Results

In this section we run some experiments to evaluate the implemented irregular morphology operators. We initially ran some experiments to empirically choose the value of $\varepsilon$, and decided to choose $\varepsilon = 0.99d$, where $d$ is the distance between samples for a regularly sampled signal. This is the value used for all experiments unless otherwise specified.

It can easily be seen that the continuous dilation of $\sin(x)$ by some SE, $G$, can be written as the following function:

$$(\sin \oplus G)(x) = \begin{cases} 1, & \text{if } \pi/2 - L/2 < x + 2\pi n \leq \pi/2 + L/2 \\ \sin(x - L/2), & \text{if } \pi/2 + L/2 < x + 2\pi n \leq \pi/2 + \pi \\ \sin(x + L/2), & \text{if } \pi/2 + \pi \quad < x + 2\pi n \leq 2\pi + \pi/2 - L/2 \end{cases} \tag{64}$$

where $n \in \mathbb{Z}$, such that one of the cases is satisfied, necessarily exists for any $x \in \mathbb{R}$ and is unique, assuming the structuring element $G$ is a line segment $[-L/2, L/2]$, where $0 \leq L \leq 2\pi$, (for $L > 2\pi$, the dilation is the constant function 1).

Figure 10 shows the result of dilating a sine-wave that is regularly, but sparsely sampled. The figure clearly shows that the irregular dilation manages to represent the actual dilation (i.e. the function describing the continuous dilation of the continuous sine-wave, $\sin \oplus G$) more accurately.

The irregular operators have two advantages that make it possible to better represent the continuous operators: Firstly, the structuring element is not limited by the sampling grid, and secondly, the dilated samples may be shifted left and right, thereby decoupling from the initial sampling positions. I.e., if a sample is needed at a certain position which was not sampled in the input, the irregular operators may insert a sample at such a position.

Figure 11 shows an example where the traditional dilation fails completely, because the size of the structuring element is smaller than the distance between samples, thus the traditional dilation leaves the signal unaffected. However, since the irregular dilation shifts samples based on the SE, the irregularly dilated signal manages to transform the signal into samples that fall near the real dilation.

In Fig. 12, the result of interpolating between the dilated samples and taking the mean square error of the interpolated signal and the continuous dilation, $\sin \oplus G$, is shown for a number of different structuring elements and sampling frequencies of the sine-wave in figures 10 and 11. Linear interpolation is used, since there are cusps in the dilated signal, meaning smooth interpolators are not well-suited. Note that this is not the interpolating function used in previous sections (i.e., Eqn. (13)). Defining a complete lattice using such a top is not straightforward. A similar experiment is performed in a previous paper [3], however due to a rounding error, the results given in that paper for large sampling distances is not correct.

In Figure 13, the results of the same experiment are shown, except the sampling density in the output adapts to the sampling distance in the input in relation to the size of the structuring element. Specifically, if the gap between input samples exceeds the size of the SE, the dilation is iterated twice, using a structuring element of half the size. This is a rather naive approach to adaptively adjusting the sample density, however it helps illustrate the potential utility of the idea. One might try to adapt the number of iterations based on more complicated criteria, also adjusting the number of iterations locally, i.e., few iterations at some parts of the signal, and many at other parts, instead of the constant number of iterations used at all samples in a given signal, that is utilized in this case.

Finally, we implemented a variant of the *parsimonious path opening* (PPO) [13]. The parsimonious path opening is an approximation of the path opening [6], which preselects one-dimensional paths, based on intensity, which are then opened. This is much faster than the regular path opening, which opens all paths, based on a set of adjacency graphs (at least conceptually), and combines the result into an opened image.

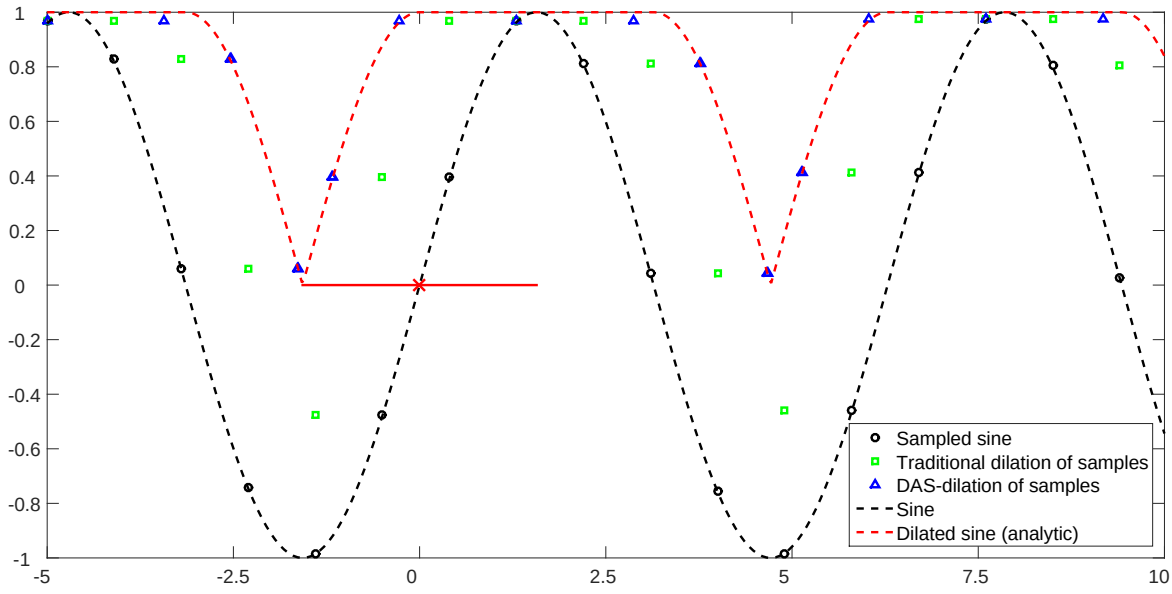


**Figure 10:** Illustration of the dilation of a regularly sampled sine-wave by the structuring element illustrated as a solid red line (the cross indicates its origin). The samples are sparse (17 samples between -5 and 10, where the value is quantized into one of 256 possible levels), which is especially problematic for the traditional dilation, which can only shift samples up or down. The structuring element used is a flat line segment of length corresponding to $\pi$. The irregular dilation proposed in this paper shifts nodes left and right, which enables a more accurate representation of the dilated signal, as evident from the figure, where the irregularly dilated samples fall very close to the analytic dilation. Note that the figure cuts off samples of the irregular dilation at positions below -5 and above 10.

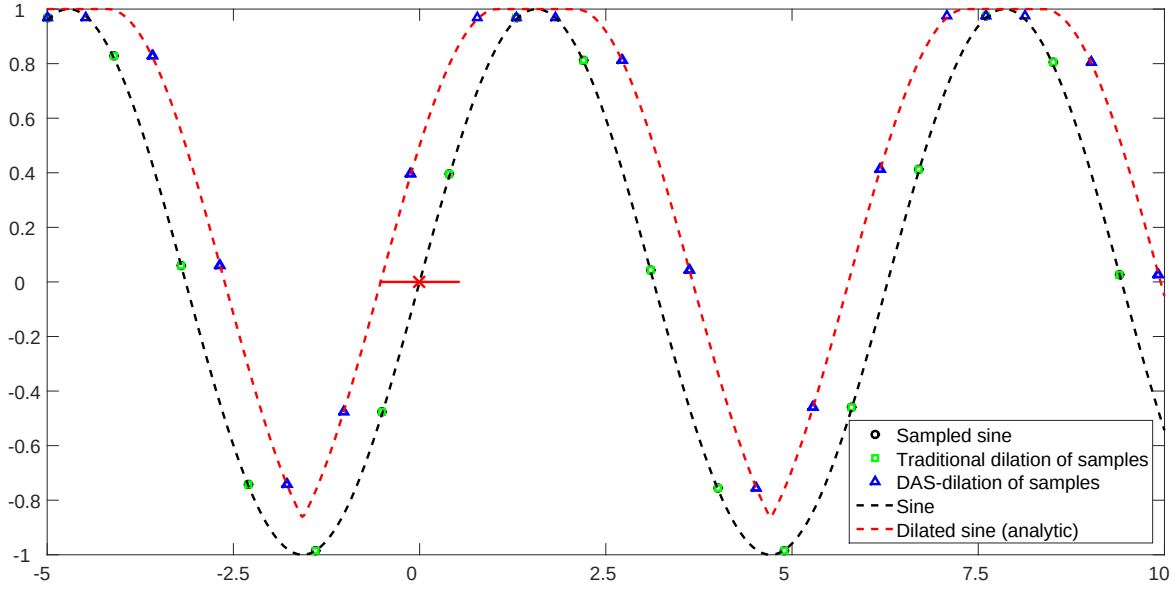


**Figure 11:** Another dilation of the sine-wave described in Figure 10 by the structuring element illustrated as a solid red line (the cross indicates its origin). This time the size of the structuring element is $\pi/3$. This means that neighboring samples are farther apart than the length of the SE, thus the traditional dilation simply returns the original samples. The irregular dilation does not require that the SE is larger than the distance between samples, since samples are duplicated and shifted. Thus, the irregular dilation gives a result that better represents the continuous operation.

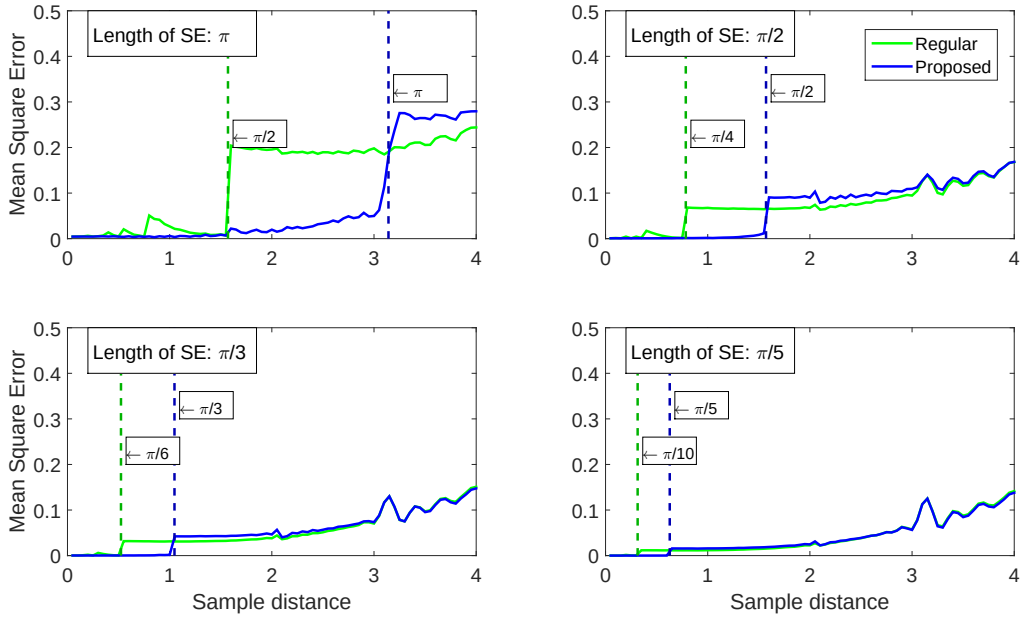


**Figure 12:** Using linear interpolation between samples in the dilations we find the mean square error for structuring elements of different lengths with increasing distance between samples when dilating the sine-wave shown in figures 10 and 11. **Green** is the error of the **traditional dilation**, and **blue** is the error of the **irregular dilation**. When the sampling distance exceeds half the length of the SE, the regular, discrete dilation becomes the identity transform, and the error increases rapidly (e.g., top left, at $\pi/2$ distance between samples marked by the green dashed line). The proposed dilation does not have this problem. When the sampling distance approaches and exceeds the size of the SE, however, the performance of the proposed dilation deteriorates because of a "staircasing" effect (e.g., top left, at $\pi$ distance between samples marked by the blue dashed line).

The PPO has a parameter $\beta$, which controls how the paths are preselected (larger values make the algorithm more robust to noise, but leave greater blind regions, through which no paths travel), we fix $\beta = 1$.

Since the parsimonious path opening extracts 1D paths, which are then opened, we can replace the 1D opening with the one proposed in this paper. We use the unbiased weights discussed in the paper by Asplund and Luengo Hendriks [1], i.e., diagonal steps have a length of $1.340$, while straight steps have a length of $0.948$. To choose $\varepsilon$, we take inspiration from our previous experiments. Since the greatest common denominator between $1340$ and $948$ is $4$, we may consider the initial irregularly sampled signal to be an element of $\mathbb{S}^{0.004}$ (i.e., $d_{\min} = 0.004$). Similarly to the previous experiments where the signals were elements of $\mathbb{S}$, we choose $\varepsilon = 0.99 \star d_{\min} = 0.99 \star 0.004$. The opening is computed by applying the proposed erosion, followed by applying the proposed dilation on the resulting dilated signal, and finally, a linear interpolation onto the original positions of the path is applied. Note that Thm. 4 does not hold in this case, because the initial erosion yields an element outside of $\mathbb{S}^{0.004}$. Moreover, the interpolation after the dilation breaks the assumption of the top being defined as in Definition 5, meaning that the proposed variant cannot, strictly speaking, be called an opening.

To evaluate this variant of the PPO, we generate four synthetic images of line segments oriented at angles between 0 and $\pi/8$. We only use two adjacency graphs, namely the south-north, and the east-west ones [13], and therefore avoid using more extreme angles in our test images. These line segments have a varying intensity $I$ such that the intensity values are given by

$$I(d) = \sin\left(\frac{n\pi d}{l}\right) + 1.5 \tag{65}$$

where $d$ is the distance from one end of the line segment, $l$ is the total length of the line segment, and $n \in \mathbb{Z}^+$ determines the number of peaks and valleys in the intensity profile. The values are then quantized so that we end up with an 8-bit image. There are ten line segments in each image, all at the same angle and with a random subpixel shift. Additionally, the line segments are given a gaussian profile with $\sigma = 1.0$ pixels. In

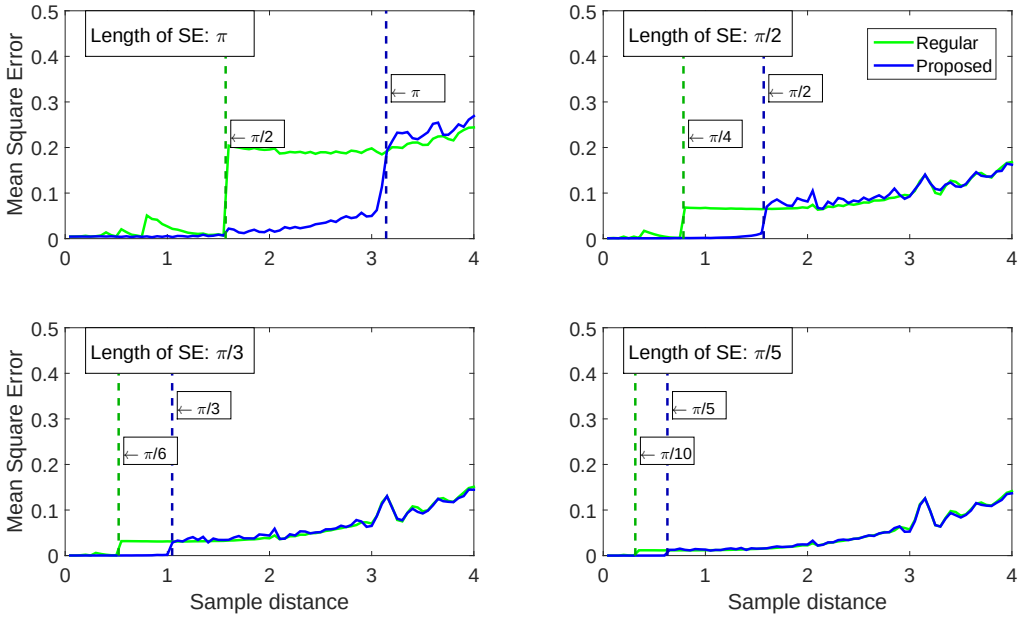


**Figure 13:** Same as Fig. 12, except we increase the sample density of the dilation when the size of the SE is smaller than the distance between input samples by performing two dilations with a SE of halved size. This naive approach to adaptively adjust sample density helps bring down the error for the proposed dilation when the distance between samples exceeds the length of the structuring element. **Green** is the error of the **traditional dilation**, and **blue** is the error of the **irregular dilation**.

this experiment we chose $l = 90$ pixels, and $n = 9$. Figure 14 shows two such test images, and a close-up of one of the line segments.

These images are then opened using a large number of line openings at angles between 0 and $\pi/8$, the final result being the supremum of these openings. The mean curve of the four cumulative length distributions computed with a granulometry using these openings, for SE lengths between 0 and 110 pixels, following reference [12], is used for comparisons (red curve in Fig. 15(c)). The images are then subsampled, keeping only a ninth of the pixels (i.e., taking every third pixel in every third row). These four subsampled images are then opened using the regular parsimonious path opening (with unbiased weights), and the variant using the opening proposed in this paper, for SE lengths in $\{0, 1/3, 2/3, \ldots, 100/3\}$.

The resulting length granulometries are shown in Fig. 15(a), and (b). The figure also shows the mean square error when comparing the mean granulometry curve (red) of the result of opening with line segments (c) as SEs (before subsampling) with the mean curve obtained using the PPO-variant (a), as well as the regular PPO (b). Also shown, for each method, is the sum of the largest absolute differences between any pair of curves (associated with a pair of angles) at each length, D, which gives an idea of the dependency on orientation. Conceptually this measures the area required for a stripe to cover the curves. Let $f_\theta(x)$ denote the value of the curve corresponding to angle $\theta$ at length value $x$, then

$$D = \int \max_{\theta,\varphi}(|f_\theta(x) - f_\varphi(x)|)\, dx \tag{66}$$

In these experiments we discretize by simply replacing the integral with a sum over the SE lengths for which the curves were computed. In the ideal case, the four curves converge to a line, meaning that the area is 0 (and consequently, $D$ is also 0). Conversely, if the result depends a lot on the orientation of the line segments, the curves will spread out, and $D$ will grow large.

It should be noted that the variant does not guarantee a non-decreasing curve. This is a result of the final interpolation as well as the issues with erosion described earlier. Overall, the PPO-variant has a better MSE, and is no worse with regard to orientation dependency.

Figure 16 shows the evolution of the error, for the same experiment, as the number of samples per line segment decreases. In this case, the error grows quicker for the PPO, than the proposed variant.

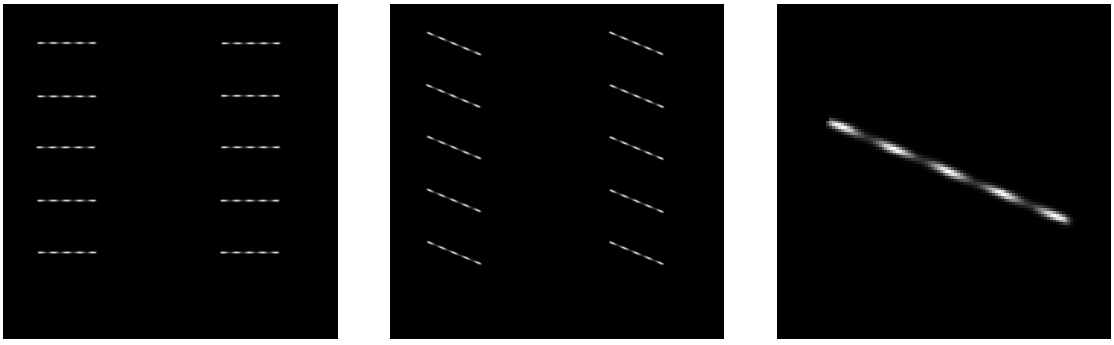

**Figure 14:** Left and middle: Examples of test images used. The test images contain 10 line segments oriented at angles between 0 and $\pi/8$, with a varying intensity. Each line segment has a gaussian profile ($\sigma = 1$) and a random subpixel shift. Right: A zoomed in view of one of the line segments.

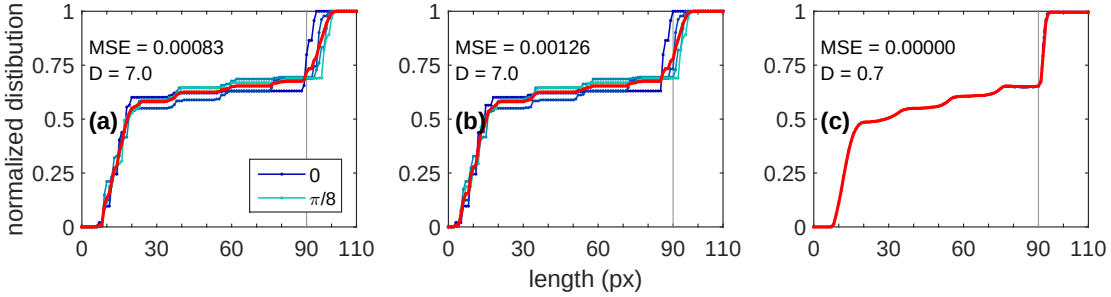


**Figure 15:** Length granulometries for the PPO-variant (a), the regular PPO (b), and the supremum over openings using straight line segments at many angles (c). The four curves in blue-teal represent the granulometry curves for the four different angles. The red curve is the mean of the four curves. The figures also display the MSE when comparing the mean curve of (a) to (c) and (b) to (c). $D$ is a measure of orientation dependency, showing the sum of differences, over each SE length, between the curve with the least value and the curve with the greatest value, meaning small values of $D$ indicate a low dependency on orientation.

Finally, we apply the PPO-variant to a real image, to show how it compares to the regular PPO. An 8-bit grayscale image of a DNA molecule on a textured background is opened using a length of 36. Figure 17 shows the result. The PPO-variant, in this case, manages to preserve the intensity of some parts of the molecule better than the regular PPO. This is consistent with the results shown in Fig. 15, where the variant better preserved the correct intensity in some cases.

# 4 Discussion

The proposed one dimensional dilation algorithm makes use of irregular sampling to better approximate the continuous dilation. If the algorithm implementation uses a self-balancing binary search tree, the dilation can be computed in $\mathcal{O}(N \log N)$ time, where $N$ is the number of input samples.

Allowing for irregular sampling means that the structuring element is no longer restricted in size by the sampling grid, thus enabling operators that work on a subpixel level, as shown in experiments. Several experiments show improved performance over the regular, discrete MM dilation for various SE sizes.

Moreover, the irregular operators are shown, experimentally, to decrease the number of samples in the output as the transformed signal becomes smoother. Some initial experiments also indicate that adaptively increasing the sampling density can lead to a better approximation of the continuous dilation.

Additionally, we replace the 1D-opening used in a path opening [6] variant, called the parsimonious path opening [13], with the opening proposed in this paper. The experiments illustrate that also in this application, the proposed irregular operators (here the openings are computed by composition) can yield improvements,

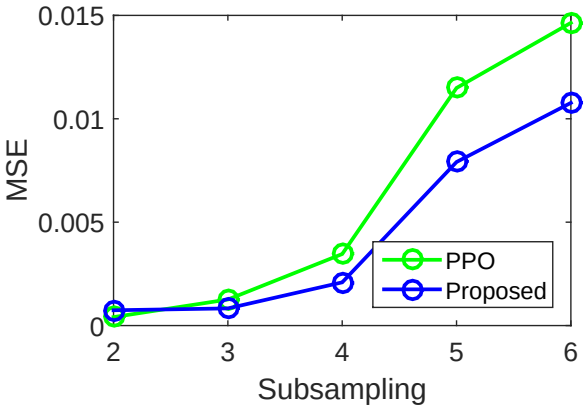


**Figure 16:** The mean square error of the average granulometry curve of PPO, and the proposed variant, compared to the curve in Fig. 15(c), as the number of samples per image segment decreases. Here a subsampling by $n$ indicates that the subsampled image contains every $n$:th pixel in every $n$:th row (the rest are discarded).

especially as the sampling frequency decreases. However, the increased accuracy comes at the cost of a less computationally efficient algorithm, since, for the original PPO, each path of $N$ pixels can be opened in $\mathcal{O}(N)$ time, instead of $\mathcal{O}(N \log N)$.

## 5 Conclusions

In this paper we present an algorithm that computes an approximation of the one dimensional continuous dilation on an irregularly sampled signal. We show that this algorithm, in one sense, performs an actual dilation under certain conditions, however, these conditions do not need to be met for an improved approximation compared to the regular, discrete dilation. From the dilation one can construct the erosion, the opening, and the closing. We provide an example of applying the proposed algorithm to compute a variant of the parsimonious path opening [13], by applying the proposed 1D dilation twice to compute the opening of the paths extracted as part of the original algorithm. This variant is shown to exhibit some desirable properties (namely in these cases better approximating the granulometry curve of images containing line segments at different orientations with varying intensities). However, this variant is slower to compute, and is not a true opening.

The operators use flat structuring elements without holes (i.e., SEs that take a constant value 0 in some interval $[a, b]$, $a, b \in \mathbb{Z}$, and $-\infty$ otherwise). Allowing for non-flat SEs should be possible by generating more samples and shifting them along the vertical axis as well as horizontally.

An initial attempt at a generalization to 2D has also been made [2], however this places some restrictions on the SEs that should be possible to ease. That paper also proposes a way of adaptively sampling signals in order to better represent parts that vary quickly, by locally increasing the sampling density, while keeping the number of samples down by decreasing the sampling density at smooth parts of the signal. This adaptive sampling could probably be incorporated into the 1D case presented here without much trouble. An initial test indicating that adaptively increasing the sampling density in the output can be beneficial in the 1D case is shown.

In this paper we also describe the problem of missing extrema in the sampling of the continuous signal, even when the sampling density is high enough to allow reconstruction of the continuous signal. It would be interesting to try to find these extrema in a preprocessing step, which would attempt to reconstruct parts of the signal that contain maxima/minima in order to be able to insert samples at the extreme points into the sampled input signal, before applying the morphological operator, thus better approximating the continuous case.

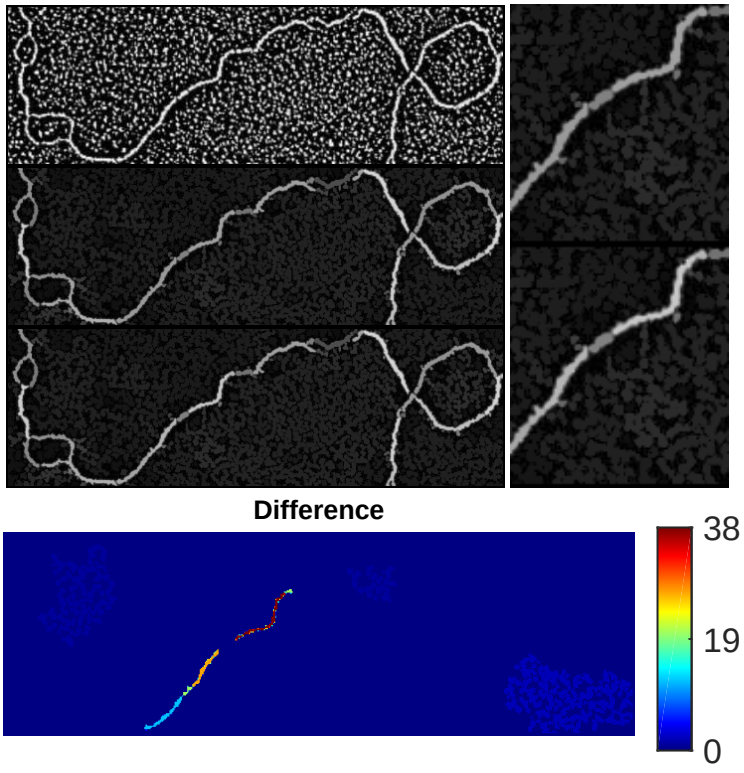


**Figure 17:** On the left side, from top to bottom: Original 8-bit image, opening using PPO (length 36), and opening using PPO variant (length 36). On the right a zoomed in view of the area containing the largest difference between the two openings is shown. At the bottom the difference between the two openings is shown using the colormap indicated by the bar on the right, in order to better illustrate the differences. Parts of the path are brighter by up to around 15% for the proposed variant.

**Acknowledgement:** Teo Asplund was funded through grant 2014-5983 from the Swedish Research Council.

# References

[1] T. Asplund and C. L. Luengo Hendriks. A faster, unbiased path opening by upper skeletonization and weighted adjacency graphs. *IEEE Transactions on Image Processing*, 25(12):5589–5600, 2016.

[2] T. Asplund, C. L. L. Hendriks, M. J. Thurley, and R. Strand. Mathematical morphology on irregularly sampled signals. In *Asian Conference on Computer Vision 2016 Workshops*, pages 506–520. Springer, 2016.

[3] T. Asplund, C. L. Luengo Hendriks, M. Thurley, and R. Strand. A new approach to mathematical morphology on one dimensional sampled signals. In *International Conference on Pattern Recognition (ICPR 2016), Cancun, Mexico, 2016*, 2016.

[4] M. Breuß and J. Weickert. Highly accurate schemes for pde-based morphology with general convex structuring elements. *International Journal of Computer Vision*, 92(2):132–145, 2011.

[5] R. W. Brockett and P. Maragos. Evolution equations for continuous-scale morphology. In *Acoustics, Speech, and Signal Processing, 1992. ICASSP-92., 1992 IEEE International Conference on*, volume 3, pages 125–128. IEEE, 1992.

[6] M. Buckley and H. Talbot. Flexible linear openings and closings. In *Mathematical Morphology and its Applications to Image and Signal Processing*, pages 109–118. Springer, 2000.

[7] S. Calderon and T. Boubekeur. Point morphology. *ACM Transactions on Graphics (TOG)*, 33(4):45, 2014.

[8] P. Dokládal and E. Dokládalová. Computationally efficient, one-pass algorithm for morphological filters. *Journal of Visual Communication and Image Representation*, 22(5):411–420, 2011.

[9] D. E. Knuth. *The art of computer programming, Volume 3: Sorting and Searching*. Addison-Wesley, 2nd edition, 1998.

[10] U. Köthe. What can we learn from discrete images about the continuous world? In *Discrete Geometry for Computer Imagery*, pages 4–19. Springer, 2008.

[11] C. L. Luengo Hendriks and L. J. van Vliet. Basic morphological operations, band-limited images and sampling. In *Scale Space Methods in Computer Vision*, pages 313–324. Springer, 2003.

[12] C. L. Luengo Hendriks, G. M. P. van Kempen, and L. J. van Vliet. Improving the accuracy of isotropic granulometries. *Pattern Recognition Letters*, 28(7):865–872, 2007.
[13] V. Morard, P. Dokládal, and E. Decencière. Parsimonious path openings and closings. *IEEE Transactions on Image Processing*, 23(4):1543–1555, 2014. 10.1109/TIP.2014.2303647.
[14] H. Nyquist. Certain topics in telegraph transmission theory. *Transactions of the AIEE*, pages 617–644, 1928. [reprinted in: Proceedings of the IEEE, vol. 90, no. 2, pp. 280-305, February 2002].
[15] G. Sapiro, R. Kimmel, D. Shaked, B. B. Kimia, and A. M. Bruckstein. Implementing continuous-scale morphology via curve evolution. *Pattern recognition*, 26(9):1363–1372, 1993.
[16] J. Serra. *Image analysis and mathematical morphology*. Academic Press, Inc., 1983.
[17] C. E. Shannon. Communication in the presence of noise. *Proceedings of the IRE*, 37(1):10–21, 1949. [reprinted in: Proceedings of the IEEE, vol. 86, no. 2, pp. 447–457, February 1998].
[18] M. J. Thurley. *Three dimensional data analysis for the separation and sizing of rock piles in mining (PhD thesis)*. Monash University, 2002.
[19] R. van den Boomgaard and A. Smeulders. The morphological structure of images: The differential equations of morphological scale-space. *Pattern Analysis and Machine Intelligence, IEEE Transactions on*, 16(11):1101–1113, 1994.
[20] J. Weickert. *Anisotropic diffusion in image processing*. Teubner Stuttgart, 1998.